Reversible down-regulation of photosystems I and II leads to fast photosynthesis recovery after long-term drought in *Jatropha curcas*

Helena Sapeta[1§], Makio Yokono[2§], Atsushi Takabayashi[3], Yoshifumi Ueno[4], André M. Cordeiro[1], Toshihiko Hara[3], Ayumi Tanaka[3], Seiji Akimoto[4], M. Margarida Oliveira[1*] and Ryouichi Tanaka[3*].

[1] Universidade Nova de Lisboa, Instituto de Tecnologia Química e Biológica António Xavier, Genomics of Plant Stress, Av. da República, 2780-157 Oeiras, Portugal

[2] Institute of Low Temperature Science, Hokkaido University, Sapporo 060-0819, Japan

[3]Division of Environmental Photobiology, National Institute for Basic Biology, Okazaki 444-8585, Japan; Department of Basic Biology, School of Life Science, the Graduate University for Advanced Studies, SOKENDAI, Okazaki 444-8585, Japan

[4] Graduate School of Science, Kobe University, Kobe 657–8501, Japan

§ equal contribution

* co-corresponding authors

Running Title: Drought-induced photoprotection includes thermal energy dissipation in both photosystems.

Highlight:

Biochemical and spectroscopic analysis of *Jatropha curcas* photosystem II and I indicates that the plant responds to extensive drought by increasing thermal dissipation of excitation energy in both photosystems.

Abstract

Jatropha curcas is a drought-tolerant plant that maintains the photosynthetic pigments under prolonged drought, and quickly regains its photosynthetic capacity when water is available. It has been reported that drought stress leads to increased thermal dissipation in photosystem (PS) II, but that of PSI has been barely investigated, one reason which could be a technical

limitation in measuring the PSI absolute quantum yield. In this study, we combined biochemical analysis and spectroscopic measurements using an integrating sphere and verified that the quantum yields of both photosystems are temporarily down-regulated under drought. We found that the decrease in the quantum yield of PSII was accompanied by a decrease in the core complexes of PSII while light-harvesting complexes are maintained under drought. In addition, in drought-treated plants, we observed a decrease in the absolute quantum yield of PSI as compared to the well-watered control, while the amount of PSI did not change, indicating that non-photochemical quenching occurs in PSI. The down-regulation of both photosystems was quickly lifted in a few days upon re-watering. Our results indicate, that in *Jatropha curcas* under drought, the down-regulation of both PSII and PSI quantum yield protects the photosynthetic machinery from uncontrolled photodamage.

Keywords: Drought; Photosynthesis; Photoprotection; Zeaxanthin; Thylakoid membrane; Photosystem I and II.

Abbreviations: A, Antheraxanthin; A_n, Net photosynthesis; β-DM, n-dodecyl β-d-maltoside; Car, Carotenoids; CEF, Cyclic electron flow; Chl, Chlorophyll; DEI, De-epoxidation index; DW, Dry weight; ETR, Electron transport rate; Fm, Maximal fluorescence; Fo, Minimal fluorescence; FR, Far red; Fv, Variable fluorescence; Fv/Fm, Maximum quantum yield of photosystem II (dark adapted); FW, Fresh weight; g_s, Stomatal conductance to water vapour; HPLC, High performance liquid chromatography; KDa, Kilodalton; LHC, Light-harvesting complex; Lhca, PSI light harvesting complex protein; Lhcb, PSII light harvesting complex protein; lpCN-PAGE, Large pore clear native - polyacrylamide gel electrophoresis; $NADP^+$, Nicotinamide adenine dinucleotide phosphate; NADPH, Reduced form of $NADP^+$; NPQ, Non-photochemical quenching; P700, PSI primary donor; $P700^+$, Oxidized PSI primary donor; ΦPSII, Quantum efficiency of PSII in the light-adapted state; PS, Photosystem; qE, Energy-dependent quenching; qI, Photoinhibitory-dependent quenching; WC, Water content; SDS-PAGE, Sodium dodecyl sulfate – polyacrylamide gel electrophoresis; V, Violaxanthin; VAZ, Violaxathin+Anthera-xanthin+Zeaxanthin; VDE, Violaxanthin de-epoxidase; Y(NPQ), quantum yield of light-

induced NPQ; Y(NO), quantum yield of non-regulated NPQ; Z, Zeaxanthin; ZE, Zeaxanthin epoxidase; ΔpH, Trans-thylakoid proton concentration gradient.

1. Introduction

Photosynthesis comprises a series of reactions that involve light-harvesting, electron transport, and the generation of a proton gradient across the thylakoid membrane. These processes require tight coordination and adjustment in response to internal and external factors such as light quantity and quality, CO_2 availability, temperature, and nutrient availability (reviewed by Nelson and Yocum, 2006; Järvi *et al.*, 2013; Colombo *et al.*, 2016; Flügge *et al.*, 2016). Under stress conditions, electron acceptors of the photosynthetic electron transport chain are often limited. Plants try to prevent impairment in electron flow through photorespiration and cyclic electron transfer, but these electron transfer pathways cannot completely remove excess electrons. Thus, suppressing charge separation is essential in preventing photo-oxidative damage. It is well known that plants down-regulate photosystem II (PSII) activity and suppress electron flow to photosystem I (PSI) (Tikkanen *et al.* 2014).

Thermal dissipation of excitation energy (non-photochemical quenching: NPQ) is essential in the down-regulation of PSII activity. Several models of thermal dissipation have been proposed in plants. Among these mechanisms, energy-dependent quenching (qE) has been the most extensively studied. In this mechanism, dynamic changes of the peripheral antenna composed of light-harvesting complexes (LHC) lead to thermal dissipation of excitation energy (Strand & Kramer 2014; Ruban 2016). These changes are induced by the pH-dependent protonation of PsbS protein (Li *et al.*, 2004). qE is also enhanced by an accumulation of zeaxanthin (Welc *et al.* 2021), which is induced by pH-dependent activation of violaxanthin de-epoxidase (VDE), an enzyme that performs the de-epoxidation of violaxanthin (V) into antheraxanthin (A) and latter zeaxanthin (Z) (the xanthophyll cycle) (Demmig *et al.* 1987). Other thermal dissipation mechanisms are also employed, especially under intensive or long stress exposure, but these are slower to relax than qE (Nilkens *et al.* 2010; Demmig-Adams *et al.* 2012; Brooks *et al.* 2013; Szymańska *et al.* 2017; Malnoë 2018). Among those, photoinhibition, or qI, has been considered as resulting from the degradation or inactivation of the D1 subunit of PSII, although these processes do not always take place concurrently (Chow *et al.* 1989). Direct energy transfer between PSII and PSI,

known as spillover, is also responsible for thermal dissipation (Yokono *et al.* 2015, 2019) and is crucial for long-term quenching in overwintering conifer needles (Bag *et al.* 2020).

The NPQ mechanisms mentioned above have been most extensively studied in model photosynthetic organisms (mainly *Arabidopsis thaliana*) under relatively short-term stresses such as several minutes to several hours of high-light exposure. Under such conditions, the major strategy to dissipate excess energy is qE quenching of PSII. However, additional mechanisms may likely be necessary to protect the photosynthetic machinery in long-term stress conditions such as drought or winter cold conditions. Several different mechanisms, including the above-mentioned spillover (Bag *et al.* 2020), phosphorylation of LHCII (Grebe *et al.* 2020), or Z accumulation (reviewed in Demmig-Adams *et al.*, 2020), have been suggested as possibly responsible for sustained NPQ in wintertime. It was also reported that D1 degradation is correlated with sustained NPQ in white pine, but not in white spruce (Merry *et al.* 2017).

It is widely accepted that thermal dissipation of excitation energy in PSI occurs when the special chlorophyll pair (P700) is oxidized (Schlodder *et al.*, 2005). This mode of quenching (P700+ quenching) is active even when the iron-sulfur clusters within PSI are damaged (Tiwari *et al.* 2016). In contrast, there are only a few reports showing evidence for thermal dissipation at PSI antennae (PSI-NPQ). Ballottari *et al*. (2014) reported that Z binding to the PSI-LHCI complex in the *npq2* Arabidopsis mutant induces rapid quenching, resulting in the apparent 30% reduction of PSI-LHCI antenna size in comparison to the wild type. However, Tian *et al*. (2017) challenged this model by reporting that they did not observe differences in the decay kinetics of PSI fluorescence between dark-adapted and high-light-adapted Arabidopsis plants. PSI-NPQ was also reported in the green alga *Chlamydomonas reinhardtii* (Girolomoni *et al.* 2019), and in the moss *Physcomitrium patens* (formerly *Physcomitrella patens*) (Pinnola *et al.* 2015). The paucity of reports on quenching in PSI antenna may be because, at room temperature, PSI emits much less fluorescence compared with PSII and it is difficult to normalize its fluorescence intensity to estimate PSI quantum yield. The studies on PSI-NPQ mentioned above analyzed time-resolved changes in absorption or fluorescence normalized either by the initial level of the signals (Ballottari *et al.* 2014; Tian *et al.* 2017) or by using a green fluorescent protein as an internal standard (Pinnola *et al.* 2015). On the other hand, an integrating sphere can monitor virtually all photons emitted from the light source and sample, making it possible to normalize the

fluorescence intensity by the number of absorbed photons. Using an integrating sphere, we have previously analyzed the absolute quantum yields of photosystems in a green alga (Ueno *et al.* 2018). The present study is the first report on the use of this technique to estimate PSI quantum yield of a drought-stressed higher plant.

Previously, we have shown that *Jatropha curcas* can withstand long periods of water withholding (up to 7 weeks) recovering photosynthetic capacity within only 3 days after rewatering (Sapeta *et al.* 2016). It is noteworthy that, unlike desiccation-tolerant plants, *J. curcas* can maintain water content during an extended drought period. Upon drought imposition, the chlorophyll (Chl) *a* to *b* ratio decreases, indicating either a decrease in the PSII core complexes or an increase in the LHCII level (Sapeta *et al.* 2013, 2016). Considering *J. curcas* quick recovery after rewatering, this response is not the consequence of uncontrolled damage, but it could be part of a regulated response to drought.

In this study, we aimed to gain insight into the mechanism that *J. curcas* uses to withstand long-term drought, focusing on the composition and response of each of its photosystems under an extended (3 weeks) drought period. We found that accompanying the decrease of Chl *a/b*, the core complexes of PSII also decrease during drought, while the levels of the PSII core complexes rapidly increase after 3 days of rewatering. A large amount of Z was found to accumulate and bind to PSII-LHCII supercomplexes and PSI-LHCI. Furthermore, using an integrating sphere, a drought-induced decrease in PSI quantum yield was observed, and fully reversible upon rewatering. These results suggest that fast thermal dissipation in PSI has physiological relevance during prolonged drought periods.

2. Materials and Methods

Plant Material

Seeds of *Jatropha curcas* were germinated in clean sand, and 10-day-old size uniform seedlings were transplanted to 2.5 L pots containing a mixture of sand, peat, and soil (2:1:1) supplemented with a commercial fertilizer (Osmocote, Scotts, Netherlands) (3.5 g/pot) (N:P:K: Mg, 16:9:12:2.5). Plants were daily irrigated until the beginning of the treatments. Experiments were carried out in a growth chamber with a 12 h photoperiod, a day/night temperature of 27.3 ± 1.6 to 24.7 ± 0.9ºC, relative humidity of 51 ± 8%, and average light intensity at plant level of ~300 µmol photon m^{-2} s^{-1}.

Drought conditions

Potted 46-day-old seedlings (six-leaf stage) were either subjected to drought imposed by water withholding (Stress) or continuously grown under well-watered conditions (Control) for all experiments except for the purification of PSI-LHCI, as described below. To assess the recovery capacity of the stressed plants, a group of plants under drought for 19 days was rewatered (Recovery). Soil water content was used to monitor stress intensity (Sapeta *et al.* 2013). Growth was monitored as described in Sapeta *et al.* (2013, 2016). For all measurements, at least three plants were used per treatment and sampling point. The experiments were performed in duplicate. A third experiment was performed for the purification of PSI-LHCI using 16-month-old potted plants and subjecting them to water withholding for 50 days.

Leaf gas exchange and Chl a fluorescence

Leaf gas exchange was assessed with a portable infrared gas analyser (LI-6400; LI-COR Inc., USA). A block temperature of 28ºC, CO_2 concentration of 400 ppm, 400 µmol photons m^{-2} s^{-1} of light intensity (10% blue and 90% red light), and an airflow rate of 300 µmol s^{-1} was used to monitor net photosynthesis (A_n, µmol CO_2 m^{-2} s^{-1}) and stomatal conductance to water vapour (g_s, mol H_2O m^{-2} s^{-1}) in fully expanded and illuminated leaves (3-4 h light photoperiod). Measurement of Chl *a* fluorescence was performed with a PAM fluorometer (PAM2000 Heinz-Walz, Germany). Plants were kept in darkness for at least 15 min before measurements. Fo (the minimum fluorescence yield measured in dark-adapted leaves) was determined with a weak measuring light (6 µmol photons m^{-2} s^{-1}) and was followed by a saturating pulse to estimate Fm (the maximum fluorescence yield measured in dark-adapted leaves). Afterward, red actinic light (450 µmol photons m^{-2} s^{-1}) was switched on, and saturating pulses were emitted (every 20 s) to estimate NPQ for a maximum period of 300 s. The fluorescence amplitude before the last saturating pulse was defined as F, and the maximum fluorescence during the last saturating pulse was defined as Fm'. Maximum variable fluorescence (Fv/Fm) was calculated as (Fm - Fo)/Fm (Kitajima & Butler 1975). The effective photochemical quantum yield of PSII (Y(II)) was calculated as (Fm'- F)/ Fm' (Genty *et al*., 1996). NPQ was calculated as [(Fm/Fm') - 1] (Bilger & Björkman 1990). Y(NPQ) representing the quantum yield of light-induced NPQ was calculated as [(F/Fm') - (F/Fm)], Y(NO) representing the quantum yield of non-regulated NPQ was calculated as

F/Fm (Genty *et al*., 1996). The coefficient of photochemical fluorescence quenching (qP) was calculated as (Fm' – F) / (Fm' – Fo) (Schreiber *et al.* 1986).

Leaf pigment composition

Two leaf discs (Ø = 19 mm) were cut from a fully expanded leaf and immediately frozen in liquid nitrogen, and pigments were extracted with chilled acetone (-30ºC) by mechanical disruption of the leaf tissue. High-performance liquid chromatography (HPLC) determinations were performed using a Hitachi model, equipped with an L-7100 pump, L-2200 sample injector, L-7300 column oven, and L-2450 diode array detector (operating in the range of 400-700 nm), and with a C18 column (YMC AL303, 5 µm particles, 250 x 4.6 mm). For all pigments except for β-carotene determination, the mobile phase (solutions A: ethanol-methanol-hexane (20:60:20, v/v/v) and B: methanol) and elution was carried out using a graded descending series of A in B (100% - 17 min, 70% - 1 min, 50% - 1 min, 20% - 1 min, 10% - 1 min and 0% - 10 min). The column was equilibrated with 100% A - 8 min. For β-carotene determinations, a second run was performed with 100% B for 13 min. Calibration curves for quantitative determinations were performed by linear regression of standard peak area *versus* the respective concentration.

Leaf water content

Leaf water content (WC) was determined as WC= [(FW - DW)/FW] x 100, six leaf discs (Ø = 19 mm) were collected for each plant from the three youngest expanded leaves (2 discs per leaf). FW represents the fresh weight of freshly cut leaf discs and DW stands for dry weight after drying the leaf discs at 50ºC (until a constant weight was achieved).

SDS-PAGE and immunoblotting

A 20 mg aliquot of grinded leaf tissue was homogenized with 200 µl of extraction buffer [100 mM Tris-HCl (pH 8), 2% SDS, 350 mM sucrose, and 20 mM DTT]. Homogenates were centrifuged at 21,600 × *g* for 5 min at 4ºC, and supernatants were used for SDS-PAGE. Leaf proteins (equivalent to 0.2 µg of Chl) were separated in 14% polyacrylamide gels, where the ratio of bisacrylamide to the total acrylamide was 2.6%. The gels were prepared using a gel buffer containing 12.4 mM Tris/HCl (pH 6.8), 0.1% SDS, and 6 M urea. After electrophoresis, one gel was stained using Coomassie Brilliant Blue (CBB) and the remaining gels were used for immunoblotting analysis. The resolved proteins were

electroblotted onto a PVDF membrane (GE Healthcare) and detected with primary antibodies as follows: anti-CP43 (Tanaka *et al.* 1991) and Agrisera's anti-CP47 (AS04 038), anti-Lhcb1 (AS01 004), anti-Lhcb2 (AS01 003), anti-PsaB (AS10 695), anti-Lhca1 (AS01 005) and anti-Lhca2 (AS01 006) antisera. Chemiluminescence signals were recorded using a LumiVision Pro 140EX (Aisin Seiki) and quantified using ImageJ (Schindelin *et al.* 2012). To determine PSII/PSI and PSII/LHCII ratios, the average band intensity of CP43 and CP47, that of Lhcb1 and Lhcb2, and that of PsaB were measured to represent PSII, LHCII, and PSI, respectively.

Thylakoid isolation

Thylakoid membranes were isolated from three fully illuminated (300 µmol photons m^{-2} s^{-1}) and expanded leaves per plant (~9 g FW) grown under control (well-watered), stress (22-days water withholding) or recovery (19-days stress + 3-days rewatering) conditions following the method of Järvi *et al.* (2011) with minor alterations. In brief, leaves were cut in small pieces (2 x 3 cm) and blended on ice-cold grinding buffer [50 mM HEPES-KOH (pH 7.5 at 4°C), 330 mM sorbitol, 2 mM EDTA, 1mM $MgCl_2$, 5 mM ascorbate, 0.05% BSA and 0.25 mg ml^{-1} Pefabloc SC as protein inhibitor]. The blended mixture was filtered through 2 layers of Miracloth and centrifuged (4,100 × *g* for 5 min at 4ºC). The pellet was gently resuspended with a brush in shock buffer [50 mM HEPES-KOH (pH 7.5 at 4°C), 5 mM sorbitol, and 5 mM $MgCl_2$], gently added to the surface of 1.5 volumes of shock buffer supplemented with 80% Percoll (v/v) and immediately centrifuged in a swing out centrifuge (1,600 × *g* for 5 min at 4ºC). The intermediate layer (above the Percoll solution) was gently collected, resuspended in shock buffer, and centrifuged (3,700 × *g* for 5 min at 4°C). The pellet was resuspended in storage buffer [50 mM HEPES-KOH (pH 7.5 at 4°C), 100 mM sorbitol, and 10 mM $MgCl_2$]. After Chl quantification (Chl was extracted with 80% acetone and determined spectrophotometrically according to Porra *et al.,* 1989), isolated thylakoids were diluted to 1 mg Chl ml^{-1} with BTH buffer [25 mM Bis-tris-HCl (pH 7.0 at 4°C), 20% glycerol (w/v), 10 mM sodium fluoride and 0.25 mg ml^{-1} Pefabloc SC], and either immediately used or stored at -196°C for future analysis.

Large pore clear native PAGE (lpCN-PAGE) fractionation of thylakoid membranes

Large pore gradient gels were prepared as previously described (Yokono *et al.* 2015). Briefly, gels included a separation gel with an acrylamide gradient (3.5-12.5%, where the ratio of bisacrylamide to the total acrylamide was 3%) and a stacking gel (3% acrylamide concentration, where the ratio of bisacrylamide to the total acrylamide was 20%). Both gels components were prepared using the same buffer [50 mM Bis-Tris/HCl (pH 7.0 at 4°C), 0.5 M 6-aminocaproic acid, and 0.05% digitonin as detergent]. The separation gel was prepared at 4ºC and polymerized at 25ºC for 3 h, the stacking gel was prepared at room temperature and polymerized for 40 min at 30°C.

Isolated thylakoids (1 mg Chl ml^{-1}) membranes were solubilized by adding an equal volume of 2% n-dodecyl β-D-maltoside (β-DM, Wako) solution on ice mixed by gentle pipetting, followed by centrifugation to remove insoluble materials (21,600 × *g* for 2 min at 4ºC). Next, 2% Amphipol A8-35 (Anatrace) was added to the supernatant (as an amphipathic surfactant to maintain membrane proteins solubilized) which was then loaded onto a gradient large-pore gel. For electrophoresis, an anode buffer [50 mM Bis-Tris/HCl (pH 7.0 at 4°C)] and a cathode buffer [50 mM Tricine, 15 mM Bis-Tris/HCl (pH 7.0 at 4°C), 0.01% Amphipol] were used according to Yokono *et al.* (2015*b*). Electrophoresis was performed at 4ºC in the dark for approximately 3 h with a gradual increase in the voltage as follows: 75 volts for 30 min, 100 volts for 30 min, 125 volts for 30 min, 150 volts for 60 min, 175 volts for 30 min, followed by 200 volts until the sample reached the end of the gel (normally 15 min) (Järvi *et al.* 2011).

PSI-LHCI purification by sucrose density gradient

PSI-LHCI was purified from 16-month-old plants under control conditions or stress (50 days of water withholding). Thylakoids were isolated as described above after adapting the plants to low-light (20 µmol photons m^{-2} s^{-1}) for 14 h. PSI-LHCI purification was performed according to Ballottari *et al.* (2004) as follows: thylakoid membranes were solubilized with 1% (w/v) β-DM and then fractionated by ultracentrifugation in a 0.1-1 M sucrose gradient supplemented with 0.06% β-DM and 5 mM Tricine, pH 7.8. After centrifugation for 21 h at 40,000 × *g* in an RPS56T rotor (Hitachi) at 4ºC, the lowest Chl-containing band was collected, and 4% (w/v) Amphipol A8-35 was added to a final concentration of 1%.

Isolated photosynthetic complexes second dimension analysis by SDS-PAGE

After electrophoresis, the lpCN–PAGE gel lanes were cut and incubated in 10% (w/v) SDS and 0.5% (w/v) 2-mercaptoethanol, at 30ºC for 50 min. A gel lane was placed horizontally over a 14% polyacrylamide with 6 M urea and subjected to conventional SDS-PAGE analysis. Staining was performed with SYPRO Ruby protein gel stain (Thermo-Fisher Scientific, USA) according to the manufacturer's protocol.

For pigment extraction of excised gel bands, gel slices were manually grinded with a pestle. A small amount of water (ca. 50 µL) was added and centrifuged twice at 4°C for 10 min at 21,600 × *g*. The supernatant was collected and 4 volumes of 100% acetone were added. Pigments were quantified by HPLC, as above described for leaf pigment determinations, with an injection volume of 60 µL.

Gel images acquisition

Gel images were captured with a scanner (GT-X970, Epson, Japan) and levels were adjusted equally among treatments (Photoshop CS5.1, Adobe Systems, USA). Gel fluorescence pictures and SYPRO Ruby stained gels were captured after excitation using a LumiVision Pro 140EX (Aisin Seiki, Japan) equipped with a custom-made LED array (466 nm, FWHM 26 nm) and a long pass optical filter (YA3 SO-56, Kenko Tokina Co., Japan).

Photosynthetic complexes spectroscopy sample collection

The fluorescence quantum yield at low temperature was measured to determine the absolute fluorescence emission of PSII and PSI complexes for control, stress, and recovery leaves. In detail, one disc (Ø = 2 cm) was collected from each leaf either adapted to dark (11 h darkness) or light (3 h under the regular photoperiod described above), transferred to the quartz tubes, and frozen within 30 s. Additionally, PSI-LHCI excised bands (from lpCN-PAGE) and fractions recovered from the sucrose density gradient were placed inside quartz tubes, immediately frozen in liquid nitrogen, and stored at −80°C before spectroscopic measurements.

Low-temperature fluorescence quantum yield

Absolute fluorescence spectra at –196ºC were measured with a spectrofluorometer equipped with an integrating sphere (JASCO FP-6600/ILFC-543L) as described by Ueno *et*

al. (2018). The excitation wavelength was 440 (mainly exciting Chl *a*) or 480 nm (mainly exciting Chl *b* and carotenoids) to distinguish the overall responses of photosystems and those of the peripheral antenna. The fluorescence intensity was normalized relative to the number of photons absorbed by each sample.

Time-resolved fluorescence analyses

Fluorescence decay-associated spectra (FDAS) were constructed as previously described (Yokono *et al.* 2008; Akimoto *et al.* 2012). In brief, time-resolved fluorescence was measured using the time-correlated single photon counting method at –196°C. The excitation wavelength was set to 408 nm and the repetition rate of the pulse trains was 2 MHz, which did not interfere with measurements taken at up to 100 ns (24.4 ps/channel × 4096 channels). To improve the time resolution, time-resolved fluorescence was also measured for up to 10 ns (2.4 ps/channel × 4096 channels). Following global analysis of the fluorescence kinetics, FDAS were constructed.

Statistical analysis

Data were subjected either to a t-test for single comparisons or Analysis of Variance (ANOVA) for multiple comparisons using the statistical software package SIGMAPLOT 11.0 (Systat Software Inc., Chicago, USA). For ANOVA, mean comparison was carried out using Tukey's multiple comparison test. Significant results were assumed for *p-value* ≤ 0.05.

3. Results

Leaf water content is maintained under drought

J. curcas plants (46-days-old) were subjected to well-watered conditions (control) or drought imposed by water withholding (stress) for 36 days (Figure 1a). After 19 days of water withholding (when the soil water content was stable, Figure S1a of the supplementary data available at JXB online) a group of plants was rewatered, to evaluate the recovery of drought-induced photosynthetic adjustments (recovery, Figure 1a). Stress application resulted in a fast decrease of soil water content (Figure S1a) and growth arrest (Figure 1c and Figure S1 b-d), nonetheless, stress had no effect on leaf water content (Figure 1b). Moreover, no visible signs of wilting or necrosis/photobleaching lesions were observed in stress leaves (day 22, Figure 1c).

Sustained down-regulation of PSII and increased NPQ occur under drought

To investigate the drought effect on leaf physiology, we monitored leaf gas exchange, and chlorophyll (Chl) fluorescence parameters (Figure 2). Stomatal conductance (g_s) and net photosynthesis (A_n) gradually decrease under drought until day 11, remaining low thereafter (Figure 2a-b). After rewatering, g_s and A_n significantly increased within 24 hours (day 20, recovery) reaching control levels within 7 days. Chl fluorescence parameters indicating the maximum quantum yield of PSII (Fv/Fm), the quantum yield of PSII (Y(II)), open PSII population (qP), thermal dissipation that is regulated in a short term (Y(NPQ) and NPQ) and constitutive thermal dissipation (Y(NO)) were calculated by measuring Chl fluorescence 5 min after dark-to-light transition (Figure 2f-h and Figure S3). Fv/Fm in the stressed plants decreased from day 10 to 17 when it reached 0.7 (Figure 2c). After day 22 Fv/Fm further decreased, reaching 0.6 by day 28, and remaining at this level even under a longer drought period (Day 58, Figure S2a). Fv/Fm decrease was due to a concomitant decrease in the maximal fluorescence (Fm, Figure 2d) and an increase in the minimal fluorescence (Fo, from 0.45 to 0.6, Figure 2e). The drought-induced Fm decrease suggests PSII photoinhibition and sustained NPQ under stress that may lead to Fm underestimation. Indeed, increased sustained quenching in the stress plants is observed from day 6 onward by the increase of heat dissipation which is not responsive to changes in light intensity, translated by the Y(NO) parameter (Figure 2g). An increase in light-induced quenching under stress is also observed by the increase of Y(NPQ) from day 4 onwards (Figure 2f). An increase in NPQ in the stress plants was also observed from day 4 to day 10 (Figure 2h). However, no major differences between control and stress plants in NPQ were observed from day 10 onwards. This lack of differences may be explained by Fm underestimation due to sustained quenching mechanisms. Moreover, a drought-induced decrease of Y(II) and qP was observed, indicating an increase in the reduced plastoquinone population (Figure S3). After rewatering, Fv/Fm and NPQ parameters in the stressed plants recovered to the control levels (Fig. 2 c-h).

Drought induces accumulation and overnight retention of zeaxanthin

Analysis of leaf photosynthetic pigment contents on day 22 revealed similar Chl contents between control, stress, and recovery plants (Figure 3a). Moreover, similar total Chl levels were observed between treatments even after a longer stress application (58 days, Figure

S2b). Chl *a* to *b* ratio was the lowest under stress, and the highest in the control, while it was intermediate during recovery, indicating changes in the peripheral antenna composition under stress and recovery (Figure 3b and Figure S4). Major differences in carotenoid content were observed for the xanthophyll cycle pigments (Figure 3, Figure S5, and S6). On day 22, an increased de-epoxidation index (DEI) of the xanthophyll cycle pigments was observed for stress leaves as compared to control both under light-adapted (0.73 in stress and 0.09 in control) and dark-adapted conditions (0.49 in stress and 0.06 in control) (Figure 3c). The observed high leaf xanthophyll DEI under stress was due to a decrease in V content, accompanied by an increase in antheraxanthin (A) and especially in Z (Figure 3d and Figure S6a-c). The xanthophyll DEI further increased, in both light- and dark-adapted stress leaves, along with stress progression (day 36, Figure S5b and day 58, Figure S2d). The changes in DEI between light and dark conditions indicate that photosynthetic electron transfer occurred and ΔpH across the thylakoid membrane is formed under light conditions in both control and stressed plants. Nevertheless, it was notable that part of the Z pool was not converted to violaxanthin (V) under dark conditions in the stressed plants. After rewatering, the DEI was restored to control levels (0.12 light and 0.08 dark, respectively). In addition to xanthophyll interconversions, the total xanthophyll pool (V+A+Z) per Chl showed a 2-fold increase under stress, suggesting that besides conversion of pre-existing V into A+Z, *de novo* synthetized Z is accumulated under stress (Figure S6d). Other carotenoids measured (lutein, neoxanthin, and β-carotene) showed no significant alterations in response to stress until day 26 (Figure S6e-g), except for an increase in neoxanthin on day 22 in the recovery plants. The reason for the change in neoxanthin content is not clear at the moment. Although it was not statistically significant, we could observe a slight increase in lutein and a decrease in β-carotene contents for stress and recovery plants on day 22, as compared to control conditions (Figure 3b), which is consistent with the observed decrease in the PSII core proteins (see below).

Drought induces reorganization of photosynthetic complexes

Thylakoid membrane protein complexes were solubilized and fractionated by large-pore clear native PAGE gel electrophoresis (lpCN-PAGE, Figure 4). It should be noted that we used wide combs (ca. 11 mm) for sample loading since a relatively large amount of uniform

protein bands was necessary for subsequent pigment extraction and spectroscopic analysis. When using wide combs, both sides of a lane tend to be distorted, thus we removed the distorted part of the gel from subsequent analysis and used only the uniform middle part of each lane (Figure 4 and Figure S7). In addition, the individual pigment composition of the most prominent complexes was quantified and the protein subunits composing each complex were assessed by denaturing SDS-PAGE. The identities of the isolated complexes shown in Figure 4a were assigned based on migration patterns, absorption and fluorescence spectra, apparent molecular weights (estimated from the second-dimension SDS-PAGE), and pigment compositions, as compared with reported data (Aro *et al.* 2004; Järvi *et al.* 2011) (for details see Appendix S1, Figure S7 and Table S1 in the Supporting Information).

In this lpCN-PAGE analysis, PSII-LHCII super-complexes (PSII-LHCIIsc) were decreased under stress in comparison with the control (Figure 4a,b). On the other hand, LHCII trimer/monomer bands increased under stress, resulting in a decreased PSII to LHCII ratio under stress (0.6 *versus* 1.1, respectively, Figure 4c). The decrease in the PSII to LHCII ratio was due to a decrease in PSII core proteins levels and an increase in Lhcb levels under stress as was assessed by immunoblotting analysis of CP43 and CP47, Lhcb 1 and 2 (Figure S8). After 3-days of rewatering, PSII-LHCIIsc levels increased toward control levels and LHCII trimer/monomer levels decreased, although LHCII trimer/monomer levels remained slightly increased in relation to the control (Figure 4a).

On the other hand, the content of the PSI-LHCI band (which was co-migrating with a minor amount of the PSII dimer) remained similar between treatments (Figure 4a), presenting similar protein content and distribution (Figure 4b) and showing similar protein levels for PsaB, Lhca1, and Lhca2 (Figure S8). Consistently, a decrease in the PSII to PSI ratio was observed under stress as compared with control (1.1 *versus* 1.4, respectively, Figure 4c).

Zeaxanthin binds the pigment-binding complexes under stress

No major variations were observed for the total Chl to total carotenoid ratio in the pigment compositions of PSII-LHCIIsc, PSI-LHCI, and LHC trimer between treatments (Figure 4d). Accordingly, similar subunit compositions in each complex were observed in control, stress, and recovery (Figure 4b). Chl *a* to *b* ratios in these complexes were overall similar between treatments(Figure 4d). On the other hand, a high DEI (≥0.7) was observed under stress for

all the isolated complexes, with DEI decreasing toward control values after 3 days of recovery (Figure 4d and Table S1). In detail, under stress, ~2.5 Z molecules were found per 100 Chls of PSII-LHCIIsc and LHCII, while ~2 Z were found per 100 Chls for the PSI-LHCI enriched band (Table S1). These amounts are higher than the reported 0.8-1.1 Z (per 100 Chls) bound to PSII-LHCIIsc and LHCII trimer (Dall'Osto *et al.*, 2012; Xu *et al.*, 2015) and ~1 Z per PSI-LHCI (Ballottari *et al.*, 2014; Tian *et al.*, 2017) reported for *A. thaliana* under high-light stress, while it was lower than the Z contents in the *npq2* Arabidopsis mutant (~3.2 Z per 100 Chl: Ballottari *et al.*, 2014).

PSII and PSI fluorescence undergoes quenching in drought conditions

To further investigate the effect of drought and subsequent recovery on light harvesting and energy distribution of both photosystems, we measured Chl fluorescence from leaves or purified PSI particles at –196ºC using an integrating sphere (JASCO FP-6600/ILFC-543L; Ueno *et al.*, 2018), which collect fluorescence emission in almost all directions (Figure 5). In this series of experiments, fluorescence emission spectra of the control, stress, and recovered leaves were obtained and normalized relative to the number of photons absorbed by each sample.

With leaf samples harvested from the control, stress, and recovery plants, three distinct peaks were observed (Figure 5), two being associated with PSII (~688 and ~697nm) and one associated with PSI (~736 nm) (Lamb *et al.* 2018). In light-adapted conditions, plants in control and recovery conditions showed similar spectra and fluorescence intensity along the whole range of wavelengths, while under stress a clear reduction in fluorescence intensity was observed for the PSI peak (35% reduction, Figure 5a). One possible explanation for this could be a relative increase in the amount of the quenched-state PSII, which would lead to an apparent decrease in the relative intensity of PSI fluorescence. However, we think this is unlikely due to the rather decreased PSII-LHCIIsc content observed in the stressed leaves in CN-PAGE analysis (Figure 4a). Another possibility is a decrease in the quantum yield of PSI in stressed leaves, as compared to control or recovered leaves.

To get further insights into the observed fluorescence decrease under stress, we compared the low-temperature fluorescence spectra of light-adapted (in which NPQ should be active) *versus* dark-adapted leaves (in which NPQ, at least the qE component, should be

462 relaxed) (Figure 5b). In the light-adapted control and recovery plants, the low-temperature
463 PSI fluorescence was higher than in dark-adapted conditions (Figure 5b). In contrast, under
464 stress, the PSI fluorescence was decreased by 18% in light-adapted conditions, as compared
465 to dark-adapted. These results suggest that the light-induced decrease in stress leaves PSI
466 quantum yield could be due to non-photochemical quenching at PSI.
467 Furthermore, we observed a slight shift to shorter wavelengths of the PSI fluorescence
468 peak in stressed plants in light conditions (from 736 to 734 nm). Taken together, these results
469 suggest that the fluorescence intensity of LHCI long-wavelength Chls (red Chls) may be
470 lowered under drought, making the PSI peak appear to be relatively shifted to a shorter
471 wavelength. Subsequently, we compared the fluorescence after excitation at 440 nm, to
472 excite Chl *a*, or 480 nm, to excite Chl *b* and carotenoids (Figure S9). In the control and
473 recovery plants, excitation at 440 or 480 nm did not show differences in the fluorescence
474 spectra, while in the stressed plants, a 13% reduction in PSI quantum yield was observed
475 when excited at 480 nm as compared with 440 nm. Thus, indicating that the excitation
476 energy was quenched within the LHC antenna, or when it was transferred from the LHC
477 antenna to PSI.
478 To further investigate the possibility that absorbed light energy is quenched at PSI, we
479 examined the fluorescence yield of isolated PSI-LHCI complexes (Figure 5c). PSI-LHCI-
480 enriched CN-PAGE gel slices containing a small amount of co-migrated PSII dimer (see
481 Figure 4a) were used for fluorescence measurements (Figure 5c). In these studies, the PSI-
482 LHCI fluorescence of the stressed plants was significantly lower than that of control or
483 recovery plants. Since the fluorescence intensity measured in the integrating sphere was
484 normalized to the number of absorbed photons, we considered the possibility that the
485 apparent decrease of PSI fluorescence in the stressed leaf samples could be influenced by
486 the comigrating PSII dimer. Therefore, to obtain a more accurate estimation of the PSI
487 fluorescence yield we further purified the PSI-LHCI fraction by ultracentrifugation in a
488 sucrose gradient. The resulting PSI fraction proved to be less contaminated with PSII, which
489 was revealed by subsequent SDS-PAGE (Figure S10c). The Z content of the purified PSI-
490 LHCI fraction was 0.9 and 2.4 for control and stressed plants, respectively. These values are
491 slightly increased as compared to those we obtained for the plants previously analysed
492 because in this experiment the plants were older. Nevertheless, we could confirm that the
493 stressed plants show a similar increase in PSI-LHCI NPQ (Figure 5d) and DEI (Figure S10d)

as compared with the plants analysed in Figure 4. This increased PSI-LHCI NPQ is visible by the 14% fluorescence reduction in stress *versus* control samples, measured with an integrating sphere (Figure 5d).

PSII quenching is 25% faster in drought-treated leaves

FDAS were constructed from the fluorescence kinetics measured at –196ºC with leaf discs collected from light-adapted plants (3 h after the onset of illumination). Six components shown in Table 1 were required to describe the fluorescence kinetics. The second component (400 ps) increased in stress compared with control (Figure 6a). In addition, the mean lifetime of illuminated leaves in the PSII wavelength region (680-690 nm) became 25% shorter in stress as compared with control (Table 1, 1.52 ns *versus* 1.14 ns, control and stress respectively). They may reflect light-dependent quenching in PSII, similar to that observed in *A. thaliana* (14%, 1.36 ns versus 1.17 ns, Yokono *et al.*, 2015*b*). On the other hand, the PSI wavelength region (730-740 nm) showed no significant difference in the mean lifetime between control and stress (Table 1) despite the decreased fluorescence yields of PSI (Figure 5). Thus, we interpreted these results as suggesting that PSI-LHCI quenching occurs under drought with a time constant shorter than the time resolution limit of our measurements, that is 5 ps.

The delayed fluorescence which originated from charge recombination at PSII showed a fluorescence peak in the wavelength region of PSI (Figure 6a, 6th components, 22-26 ns), indicating that *J. curcas* could transfer excitation energy from PSII to PSI which is termed spillover. We calculated the amount of spillover based on the delayed fluorescence at the PSI region by assuming that the contribution of the PSII vibrational band to the fluorescence at the PSI region is 15% (Yokono *et al.* 2015). Under this assumption, we estimated that similar amounts of PSII excitation energy (about 60%) are transferred to PSI under both control and stress conditions (Table 1). Thus, we conclude that the regulation of spillover does not account for an increase in NPQ under drought.

Fluorescence decay curves (Figure 6b) were reconstructed from the FDAS data shown in Figure 6, and the results of the integrating sphere shown in Figure 5a. In the LHC (683 nm) and PSII (688 nm) wavelength regions, a slight enhancement of the fastest decay component was observed in the stressed leaves as compared to the control ones (Figure 6b), which may reflect enhanced NPQ in PSII. On the other hand, in the PSI wavelength region

(738 nm), a substantial reduction (~50%) in fluorescence rise which is shown as negative amplitudes was observed in stressed leaves. Interestingly, the fluorescence intensity at time 0 was almost the same between control and stressed leaves, suggesting that the amount of absorbed energy by PSI was similar, which is consistent with the similar PsaB levels under stress and control conditions (Figure S8). Except for the early fluorescence rise, no major differences in fluorescence decay were observed between control and stress at 738 nm, although the decay was slightly faster in the control (Figure 6b). The decreased fluorescence rise of PSI in stress can be explained by decreased energy transfer from LHC and/or PSII to PSI. However, this hypothesis is unlikely because few differences were observed in the LHC and PSII wavelength regions (Figure 6a, approximately 690 nm). A more likely explanation is PSI quenching with a time constant equal to (or faster than) PSI red Chl energy acceptation (<30 ps). Thus, we suggest that *Jatropha curcas* PSI performs fast non-photochemical quenching under drought conditions.

4. Discussion

Jatropha curcas presents a water conservation strategy under water-limiting conditions, with strict stomatal closure to avoid water loss through transpiration. Although stomatal closure is an efficient strategy to reduce water loss, it also reduces CO_2 availability, thus limiting CO_2 fixation and increasing the chances of photooxidation. Under such conditions, photorespiration and cyclic electron transfer are enhanced to alleviate a limitation in electron acceptors (Golding & Johnson 2003; Kohzuma *et al.* 2009; Zivcak *et al.* 2013; Lima Neto *et al.* 2017). Nevertheless, it should be essential to down-regulate excitation energy transfer to the reaction center to decrease the overall photosynthetic electron flow.

We found that increased NPQ under drought was composed of flexible components, which are rapidly induced/relaxed in response to light, as well as sustained components that remain active in the dark (Figure 2). In this study, sustained NPQ was shown by the sustained decrease of Fv/Fm, increased Y(NO), and overnight Z-retention under drought. Sustained quenching was previously reported for other species subjected to severe and extended stress, such as evergreen conifers at sub-zero temperatures in wintertime (reviewed by Verhoeven, 2014; Bag et al. 2020)) and *Quercus* species under summer drought (Peguero-Pina *et al.* 2009). We show that sustained quenching has major physiological

relevance under prolonged drought exposure, allowing a "locked-in" photoprotection state and preventing damaging reactions that may occur when qE has not yet been activated (e.g. in the beginning of the light period). Moreover, sustained PSII quenching ensures the maintenance of a low electron flow to PSI in the absence of qE, thus preventing PSI photodamage (Tikkanen *et al.*, 2014). In evergreen trees, it was recently proposed that sustained NPQ was controlled by the phosphorylation of LHC (Grebe *et al.* 2020) and direct energy transfer from PSII to PSI (Bag *et al.* 2020). In these trees, photoinhibition may also occur, but a decrease in the reaction center complexes is not significant (Grebe *et al.* 2020; Bag *et al.* 2020). In contrast, in the case of *J. curcas*, photoinhibition (degradation of the PSII core complex) seems to play a major role in drought response, as we observed a striking decrease in Chl *a/b* ratios which is consistent with the decrease of PSII-LHCIIsc (Figure 4) and the amount of PSII CP43 and CP47 subunits (Figure S8). Upon rewatering, Chl *a/b* ratios and the PSII-LHCIIsc gradually recovered (Figs. 3 and 4, and Figure S8) which agrees with the recovery of photosynthetic activity (Figure 2). The results indicate that a decrease in PSII-LHCIIsc coincided with the down-regulation of PSII (Figure 2d). In a typical form of photoinhibition, D1 is inactivated without apparent loss of the reaction center. In such a case, charge recombination between Q_A and $P680^+$ may lead to thermal dissipation of the excitation energy, or it was recently suggested that some oxidized chlorophyll molecules in the reaction center complex may quench the excitation energy (Nawrocki *et al.* 2021). On the other hand, since the reaction center complex was significantly decreased in stressed *J. curcas* plants, thermal dissipation at the peripheral antennae of PSII may dominate.

A marked increase in the Z content and DEI was observed in stressed plants likely contributing to increased qE quenching by allosterically changing LHC structure (reviewed by Horton, 2014; Ruban and Mullineaux, 2014). In addition to the alterations in the DEI, the total leaf VAZ pool was found to be doubled under stress (mainly due to increased Z). This indicates that besides de-epoxidation of V to Z bound to LHC proteins, extra Z is accumulated. Similarly, an increased VAZ pool under drought was reported for other species (summarized by meta-analysis studies by Wujeska *et al.*, 2013 and Esteban *et al.*, 2015). An increase in Z contents by treatment of a chemical plant growth regulator, paclobutrazol, results in drought tolerance in *Quercus ilex* and *Q. robur* (Percival & AlBalushi 2007). Likewise, it was reported that overexpression of β-carotene hydroxylase led to an increase in the VAZ pool and drought tolerance in Tobacco plants, indicating that

588 an increase in Z contents significantly contributes to drought tolerance (Zhao *et al.* 2014).
589 Though current data does not allow us to clarify the role of Z in drought tolerance, we
590 hypothesize that extra Z might localize in the lipid phase, where it can act as an antioxidant
591 (Havaux *et al.* 2007) and/or increase membrane stability (Havaux 1998). Otherwise, extra
592 Z may participate in NPQ without requiring defined binding positions, as it may be trapped
593 in between the antenna proteins contributing to NPQ due to the proximity to the antenna
594 exposed Chls, as suggested by Xu *et al.* (2015).
595 We further found that the quantum yield of PSI decreased by about 30% in the stressed
596 leaves as compared to control or recovered leaves (Figures 5a and 5b). In these
597 measurements, an integrating sphere captured all photons emitted, and the fluorescence
598 intensity was normalized to the total photons absorbed. A possible explanation for a
599 decrease in PSI fluorescence could be that the photon absorption by PSII and/or LHCII have
600 increased under drought conditions. However, we think this is unlikely because PSII was
601 decreased under drought while the PSI levels were relatively constant in all treatments
602 (Figures 4 and S8). Moreover, the purified PSI fraction also showed a decrease in its
603 quantum yield (Figure 5d). These results suggest that the excited energy is to some extent
604 quenched at PSI.
605 The fluorescence decay curves of the control and stressed plants at 738 nm which
606 represents the fluorescence from PSI were similar except that the initial rise of Chl
607 fluorescence was substantially suppressed in the stressed plants (Figure 6). This suggests
608 that the quenching occurs very fast, probably faster than ~10 ps. Since the long-wavelength
609 fluorescence (~738 nm) is assumed to be originated from Chl pairs of low-energy states
610 (red-shifted Chl), which are most likely located at LHCI (Jennings *et al.* 2004; Qin *et al.*
611 2015), we speculate that the excited energy is quenched nearby the red-shifted Chl. The
612 exact mechanism behind our observed decrease in PSI fluorescence is not clear at present,
613 but a possible mechanism is that Z induces structural changes in PSI, or that Z forms a
614 quenching site in the stressed leaves. Both hypotheses are in line with our observations that
615 the fluorescence reduction and Z accumulation are reversible upon rewatering (Figure 5a
616 and Table S1).
617 Excitation energy quenching at PSI was also reported by Ballottari and colleagues
618 (Ballottari *et al.*, 2014). These authors analyzed the FDAS of the Z accumulating *npq2*
619 Arabidopsis mutant and showed that the second fastest component among their observed

FDAS was shortened from 18 ps in the wild type to 12 ps in the *npq2* mutant. They suggested that some Z molecules bound to the interphase of PSI-LHC could be responsible for quenching. This hypothesis is consistent with our observation, except that in *J. curcas*, PSI-LHCI quenching can be even faster. In contrast, Tien *et al*. (2017) reported that fluorescence decay kinetics of PSI-LHCI were identical in the *A. thaliana* plants grown under low- and high-light conditions, where they predominantly accumulated V and Z, respectively. The reason for this discrepancy is not clear at present, but in the report of Tien *et al*. (2017), only one-third of V binding sites were replaced with Z even under high-light conditions, while in the *npq2* mutant, all V molecules were replaced by Z. We speculate that more extensive binding of Z to PSI-LHCI may be necessary to induce PSI quenching, as we observed in the stressed *J. curcas* leaves.

PSI quenching has also been reported in algae and moss. In the green alga, *Chlorella vulgaris,* Z binding decreased the average fluorescence lifetime of an isolated PSI complex from 72 ps to 49 ps (Girolomoni *et al.* 2020). In *Physcomitrium patens*, high-light-treated (high NPQ) chloroplasts presented a strong decrease of low-temperature PSI fluorescence (in comparison to dark-adapted chloroplasts, *i.e.* unquenched state) (Pinnola *et al.* 2015). These authors found that PSI fluorescence quenching was due to the action of an LHCSR (light-harvesting complex stress-related protein, a pH-sensing protein involved in the qE component of NPQ in green algae) and LHCII connected to PSI. The same research group also reported LHCSR-dependent PSI quenching in *C. reinhardtii* (Girolomoni *et al.* 2019). In this case, the change occurred at a relatively slow range: the constant of one of the decay-associated components that fitted the PSI spectrum changed from 1.72 ns to 1.29 ns when high-light was imposed on WT cells.

PSI is recognized as more resilient to photodamage than PSII, but it can be also photoinhibited when the electron flow from PSII exceeds the availability of electron acceptors (Hihara and Sonoike, 2001; Sonoike, 2011). Under drought, a decrease in electron acceptors is expected since CO_2 assimilation is largely decreased and NADPH is expected to accumulate. In such conditions, CEF around PSI is expected to be increased to reduce the possibility that electrons accumulate in Fe-S clusters in PSI. Nevertheless, electrons may eventually return to reduce P700 which will be a potential risk for PSI photoinhibition. Under such conditions, rapid quenching at PSI may decrease the risk of PSI photoinhibition.

Thus, we suggest that the concomitant operation of CEF and PSI quenching is important for the protection of the photosynthetic apparatus under long-term drought conditions.

It is known that the oxidized form of P700 ($P700^+$) is a potent quencher of excited energy (Shubin *et al.* 1995; Trissl 1997; Schlodder *et al.* 2007; Tiwari *et al.* 2016; Yokono *et al.* 2019). Nevertheless, it is unlikely that $P700^+$ is responsible for the observed decrease in the quantum yield of PSI under drought, because the energy transfer between the red-shifted Chl and $P700^+$ is relatively slow at the range of a few hundred picoseconds (Shubin *et al.* 1995; Yokono *et al.* 2019), while we did not observe significant changes in the components of fluorescence decay in this time range at around 730 nm where the red-shifted Chl emits fluorescence (Figure 6).

We show here that under long-term drought, both PSII and PSI have enhanced NPQ energy dissipation capacity, which helps the plant to protect the photosynthetic machinery from long-term drought damages and improves recovery. PSI photoinhibition could largely compromise the recovery capacity after stress relief because PSI repair would require the *de novo* synthesis and assembly, a slow process requiring several days to complete (Zhang & Scheller 2004; Sonoike 2011). Moreover, this increased PSI-NPQ capacity may contribute to dissipate the energy transferred from PSII by spillover, thus increasing the protection against photodamage of the entire thylakoid binding complexes.

Altogether, our data shows that flexible and sustained down-regulation of PSII is employed under drought, involving the reorganization of PSII-LHCIIsc. Concomitantly, we observed a drastic increase in the Z levels as well as enhanced thermal dissipation in PSI. After rewatering, the relaxation of the quenching mechanisms and the readjustment of the photosystems stoichiometry allow the photosynthesis and growth of *J. curcas* plants to be rapidly resumed.

5. Supplementary data

The following supplementary data are available at JXB online.

Figure S1. Effect of drought and rewatering on soil water content and plant growth.

Figure S2. Effect of prolonged drought and rewatering on Chl *a* fluorescence and leaf pigment composition.

Figure S3. Effect of drought and rewatering on Y(II) and qP.

Figure S4. Effect of drought and rewatering on Chl content.

Figure S5. Effect of drought and rewatering on leaf xanthophyll de-epoxidation index.

Figure S6. Effect of drought and rewatering on carotenoid content of light-adapted leaves.

Figure S7. Steady-state relative absorption and fluorescence emission spectra of major bands isolated by lpCN-PAGE.

Figure S8. Drought-induced changes in the protein levels of photosystems I and II.

Figure S9. Effect of drought on PSII and PSI low-temperature fluorescence quantum yield after excitation with 440 nm and 480 nm.

Figure S10. Purification of PSI-LHCI by sucrose-density ultracentrifugation followed by CN-PAGE.

Table S1. Pigment composition of isolated photosynthetic complexes by lpCN-PAGE for plants subjected to control, stress, and recovery at day 22.

Appendix S1 Identities of the isolated photosynthetic complexes shown in Fig. 4

6. Acknowledgments

We acknowledge funding from the Japan Society for the Promotion of Science (JSPS) through the KAKENHI Grant Number 16K21737 for HS, 16H06554, and 20H03017 for RT, and 16H06553 for SA, respectively. This work has also been supported by "Fundação para a Ciência e a Tecnologia" through the R&D Unit GREEN-IT Bioresources for Sustainability (UID/Multi/04551/2013 and UID/04551/2020). HS acknowledges FCT/MCTES funding from Ph.D. fellowship SFRH/BD/89781/2012 and PTDC/BIA-FBT/29704/2017 (co-financed by FEDER in the scope of POR Lisboa 2020). Professor Roberta Croce (Vrije Universiteit Amsterdam, The Netherlands) is acknowledged for fruitful discussions at Kurashiki.

7. Author contributions

RT, AT, TH and MMO supervised the research. HS, MY, AT, SA, and RT designed the experiments; HS, MY, YU, AMC, and RT performed the research; HS, MY, and RT analyzed the data; HS, MY, RT, SA, and MMO wrote the manuscript and all authors discussed and improved the manuscript.

References

Akimoto S., Yokono M., Hamada F., Teshigahara A., Aikawa S. & Kondo A. (2012) Adaptation of light-harvesting systems of Arthrospira platensis to light conditions, probed by time-resolved fluorescence spectroscopy. *Biochimica et Biophysica Acta (BBA) - Bioenergetics* **1817**, 1483–1489.

Aro E.-M., Suorsa M., Rokka A., Allahverdiyeva Y., Paakkarinen V., Saleem A., … Rintamäki E. (2004) Dynamics of photosystem II: a proteomic approach to thylakoid protein complexes. *Journal of Experimental Botany* **56**, 347–356.

Bag P., Chukhutsina V., Zhang Z., Paul S., Ivanov A.G., Shutova T., … Jansson S. (2020) Direct energy transfer from photosystem II to photosystem I confers winter sustainability in Scots Pine. *Nature Communications* **11**, 1–13.

Ballottari M., Alcocer M.J.P., D'Andrea C., Viola D., Ahn T.K., Petrozza A., … Bassi R. (2014) Regulation of photosystem I light harvesting by zeaxanthin. *Proceedings of the National Academy of Sciences* **111**, E2431–E2438.

Ballottari M., Govoni C., Caffarri S. & Morosinotto T. (2004) Stoichiometry of LHCI antenna polypeptides and characterization of gap and linker pigments in higher plants Photosystem I. *European Journal of Biochemistry* **271**, 4659–4665.

Bilger W. & Björkman O. (1990) Role of the xanthophyll cycle in photoprotection elucidated by measurements of light-induced absorbance changes, fluorescence and photosynthesis in leaves of Hedera canariensis. *Photosynthesis Research 1990 25:3* **25**, 173–185.

Brooks M.D., Sylak-Glassman E.J., Fleming G.R. & Niyogi K.K. (2013) A thioredoxin-like/β-propeller protein maintains the efficiency of light harvesting in Arabidopsis. *Proceedings of the National Academy of Sciences of the United States of America* **110**, E2733-40.

Chow W.S., Osmond C.B. & Huang L.K. (1989) Photosystem II function and herbicide binding sites during photoinhibition of spinach chloroplasts in-vivo and in-vitro. *Photosynthesis Research* **21**, 17–26.

Colombo M., Suorsa M., Rossi F., Ferrari R., Tadini L., Barbato R. & Pesaresi P. (2016) Photosynthesis control: An underrated short-term regulatory mechanism essential for plant viability. *Plant Signaling and Behavior* **11**, e1165382.

Dall'Osto L., Holt N.E., Kaligotla S., Fuciman M., Cazzaniga S., Carbonera D., … Bassi R. (2012) Zeaxanthin protects plant photosynthesis by modulating chlorophyll triplet yield in specific light-harvesting antenna subunits. *The Journal of biological chemistry* **287**, 41820–34.

Demmig-Adams B., Cohu C.M., Muller O. & Adams W.W. (2012) Modulation of photosynthetic energy conversion efficiency in nature: from seconds to seasons. *Photosynthesis Research* **113**, 75–88.

Demmig-Adams B., Stewart J.J., López-Pozo M., Polutchko S.K. & Adams W.W. (2020) Zeaxanthin, a Molecule for Photoprotection in Many Different Environments. *Molecules 2020, Vol. 25, Page 5825* **25**, 5825.

Demmig B., Winter K., Krüger A. & Czygan F.C. (1987) Photoinhibition and zeaxanthin formation in intact leaves : a possible role of the xanthophyll cycle in the dissipation of

excess light energy. *Plant Physiology* **84**, 218–224.

Esteban R., Barrutia O., Artetxe U., Fernández-Marín B., Hernández A. & García-Plazaola J.I. (2015) Internal and external factors affecting photosynthetic pigment composition in plants: A meta-analytical approach. *New Phytologist* **206**, 268–280.

Flügge U.-I., Westhoff P. & Leister D. (2016) Recent advances in understanding photosynthesis. *F1000Research* **5**, 2890.

Genty B., Harbinson J., Cailly A.L., Rizza F. (1996) Fate of excitation at PS II in leaves: the non-photochemical side. Presented at The Third BBSRC Robert Hill Symposium on Photosynthesis, March 31 to April 3, University of Sheffield, Department of Molecular Biology and Biotechnology, Western Bank, Sheffield, UK, Abstract no. P28, 1996.

Girolomoni L., Bellamoli F., de la Cruz Valbuena G., Perozeni F., D'Andrea C., Cerullo G., … Ballottari M. (2020) Evolutionary divergence of photoprotection in the green algal lineage: a plant-like violaxanthin de-epoxidase enzyme activates the xanthophyll cycle in the green alga Chlorella vulgaris modulating photoprotection. *New Phytologist* **228**, 136–150.

Girolomoni L., Cazzaniga S., Pinnola A., Perozeni F., Ballottari M. & Bassi R. (2019) LHCSR3 is a nonphotochemical quencher of both photosystems in Chlamydomonas reinhardtii. *Proceedings of the National Academy of Sciences of the United States of America* **116**, 4212–4217.

Golding A.J. & Johnson G.N. (2003) Down-regulation of linear and activation of cyclic electron transport during drought. *Planta* **218**, 107–114.

Grebe S., Trotta A., Bajwa A.A., Mancini I., Bag P., Jansson S., … Aro E.M. (2020) Specific thylakoid protein phosphorylations are prerequisites for overwintering of Norway spruce (Picea abies) photosynthesis. *Proceedings of the National Academy of Sciences of the United States of America* **117**, 17499–17509.

Havaux M. (1998) Carotenoids as membrane stabilizers in chloroplasts. *Trends in Plant Science* **3**, 147–151.

Havaux M., Dall'osto L., Bassi R. & Rank B. (2007) Zeaxanthin has enhanced antioxidant capacity with respect to all other xanthophylls in Arabidopsis leaves and functions independent of binding to PSII antennae. *Plant Physiology* **145**, 1506–20.

Hihara Y. & Sonoike K. (2001) Regulation, inhibition and protection of photosystem I. Kluwer Academic Publishers, Dordrecht.

Horton P. (2014) Developments in Research on Non-Photochemical Fluorescence Quenching: Emergence of Key Ideas, Theories and Experimental Approaches. pp. 73–95. Springer, Dordrecht.

Järvi S., Gollan P.J. & Aro E.-M. (2013) Understanding the roles of the thylakoid lumen in photosynthesis regulation. *Frontiers in Plant Science* **4**, 434.

Järvi S., Suorsa M., Paakkarinen V. & Aro E.-M. (2011) Optimized native gel systems for separation of thylakoid protein complexes: novel super- and mega-complexes. *The Biochemical journal* **439**, 207–14.

Jennings R.C., Zucchelli G., Engelmann E. & Garlaschi F.M. (2004) The long-wavelength chlorophyll states of plant LHCI at room temperature: A comparison with PSI-LHCI.

Biophysical Journal **87**, 488–497.

Kitajima M. & Butler W.L. (1975) Quenching of chlorophyll fluorescence and primary photochemistry in chloroplasts by dibromothymoquinone. *Biochimica et biophysica acta* **376**, 105–115.

Kohzuma K., Cruz J.A., Akashi K., Hoshiyasu S., Munekage Y.N., Yokota A. & Kramer D.M. (2009) The long-term responses of the photosynthetic proton circuit to drought. *Plant, Cell and Environment* **32**, 209–219.

Lamb J.J., Røkke G. & Hohmann-Marriott M.F. (2018) Chlorophyll fluorescence emission spectroscopy of oxygenic organisms at 77 K. *Photosynthetica* **56**, 105–124.

Li X.-P., Gilmore A.M., Caffarri S., Bassi R., Golan T., Kramer D. & Niyogi K.K. (2004) Regulation of photosynthetic light harvesting involves intrathylakoid lumen pH sensing by the PsbS protein. *The Journal of biological chemistry* **279**, 22866–74.

Lima Neto M.C., Cerqueira J.V.A., da Cunha J.R., Ribeiro R. V. & Silveira J.A.G. (2017) Cyclic electron flow, NPQ and photorespiration are crucial for the establishment of young plants of Ricinus communis and Jatropha curcas exposed to drought. *Plant Biology* **19**, 650–659.

Malnoë A. (2018) Photoinhibition or photoprotection of photosynthesis? Update on the (newly termed) sustained quenching component qH. *Environmental and Experimental Botany* **154**, 123–133.

Merry R., Jerrard J., Frebault J. & Verhoeven A. (2017) A comparison of pine and spruce in recovery from winter stress; changes in recovery kinetics, and the abundance and phosphorylation status of photosynthetic proteins during winter. *Tree Physiology* **37**, 1239–1250.

Nawrocki W.J., Liu X., Raber B., Hu C., De Vitry C., Bennett D.I.G. & Croce R. (2021) Molecular origins of induction and loss of photoinhibition-related energy dissipation qI. *Science Advances* **7**, 55.

Nelson N. & Yocum C.F. (2006) Structure of photosystems I and II. *Annual Review of Plant Biology* **57**, 521–565.

Nilkens M., Kress E., Lambrev P., Miloslavina Y., Müller M., Holzwarth A.R. & Jahns P. (2010) Identification of a slowly inducible zeaxanthin-dependent component of non-photochemical quenching of chlorophyll fluorescence generated under steady-state conditions in Arabidopsis. *Biochimica et Biophysica Acta (BBA) - Bioenergetics* **1797**, 466–475.

Peguero-Pina J.J., Sancho-Knapik D., Morales F., Flexas J. & Gil-Pelegrin E. (2009) Differential photosynthetic performance and photoprotection mechanisms of three Mediterranean evergreen oaks under severe drought stress. *Functional Plant Biology* **36**, 453–462.

Percival G.C. & AlBalushi A.M.S. (2007) Paclobutrazol-induced drought tolerance in containerized English and evergreen oak. *Arboriculture and Urban Forestry* **33**, 397–409.

Pinnola A., Cazzaniga S., Alboresi A., Nevo R., Levin-Zaidman S., Reich Z. & Bassi R. (2015) Light-harvesting complex stress-related proteins catalyze excess energy dissipation in both photosystems of Physcomitrella patens. *The Plant Cell* **27**, 3213–27.

Porra R.J., Thompson W.A. & Kriedemann P.E. (1989) Determination of accurate extinction coefficients and simultaneous equations for assaying chlorophylls a and b extracted with four different solvents: verification of the concentration of chlorophyll standards by atomic

absorption spectroscopy. *Biochimica et Biophysica Acta (BBA) - Bioenergetics* **975**, 384–394.

Qin X., Suga M., Kuang T. & Shen J.R. (2015) Structural basis for energy transfer pathways in the plant PSI-LHCI supercomplex. *Science* **348**, 989–995.

Ruban A. V. (2016) Nonphotochemical Chlorophyll Fluorescence Quenching: Mechanism and Effectiveness in Protecting Plants from Photodamage. *Plant Physiology* **170**.

Ruban A. V. & Mullineaux C.W. (2014) Non-Photochemical Fluorescence Quenching and the Dynamics of Photosystem II Structure. pp. 373–386. Springer, Dordrecht.

Sapeta H., Costa J.M., Lourenço T., Maroco J., van der Linde P. & Oliveira M.M. (2013) Drought stress response in Jatropha curcas: Growth and physiology. *Environmental and Experimental Botany* **85**.

Sapeta H., Lourenço T., Lorenz S., Grumaz C., Kirstahler P., Barros P.M., … Oliveira M.M. (2016) Transcriptomics and physiological analyses reveal co-ordinated alteration of metabolic pathways in Jatropha curcas drought tolerance. *Journal of Experimental Botany* **67**.

Schindelin J., Arganda-Carreras I., Frise E., Kaynig V., Longair M., Pietzsch T., … Cardona A. (2012) Fiji: An open-source platform for biological-image analysis. *Nature Methods* **9**, 676–682.

Schlodder E., Çetin M., Byrdin M., Terekhova I. V. & Karapetyan N. V. (2005) P700+-and3P700-induced quenching of the fluorescence at 760 nm in trimeric Photosystem I complexes from the cyanobacterium Arthrospira platensis. *Biochimica et Biophysica Acta - Bioenergetics* **1706**, 53–67.

Schlodder E., Shubin V. V., El-Mohsnawy E., Roegner M. & Karapetyan N. V. (2007) Steady-state and transient polarized absorption spectroscopy of photosytem I complexes from the cyanobacteria Arthrospira platensis and Thermosynechococcus elongatus. *Biochimica et Biophysica Acta - Bioenergetics* **1767**, 732–741.

Schreiber U., Schliwa U. & Bilger W. (1986) Continuous recording of photochemical and non-photochemical chlorophyll fluorescence quenching with a new type of modulation fluorometer. *Photosynthesis Research 1986 10:1* **10**, 51–62.

Shubin V.V., Bezsmertnaya I.N. & Karapetyan N.V. (1995) Efficient energy transfer from the long-wavelength antenna chlorophylls to P700 in photosystem I complexes from Spirulina platensis. *Journal of Photochemistry and Photobiology B: Biology* **30**, 153–160.

Sonoike K. (2011) Photoinhibition of photosystem I. *Physiologia Plantarum* **142**, 56–64.

Strand D.D. & Kramer D.M. (2014) Control of Non-Photochemical Exciton Quenching by the Proton Circuit of Photosynthesis. In *Non-Photochemical Quenching and Energy Dissipation in Plants*. pp. 387–408. Springer, Dordrecht.

Szymańska R., Ślesak I., Orzechowska A. & Kruk J. (2017) Physiological and biochemical responses to high light and temperature stress in plants. *Environmental and Experimental Botany* **139**, 165–177.

Tanaka A., Yamamoto Y. & Tsuji H. (1991) Formation of Chlorophyll-Protein Complexes during Greening. 2. Redistribution of Chlorophyll among Apoproteins. *Plant and Cell Physiology* **32**, 195–204.

Tian L., Xu P., Chukhutsina V.U., Holzwarth A.R. & Croce R. (2017) Zeaxanthin-dependent nonphotochemical quenching does not occur in photosystem I in the higher plant Arabidopsis thaliana. *Proceedings of the National Academy of Sciences of the United States of America* **114**, 4828–4832.

Tikkanen M., Rao Mekala N. & Aro E.-M. (2014) Photosystem II photoinhibition-repair cycle protects Photosystem I from irreversible damage. *BBA - Bioenergetics* **1837**, 210–215.

Tiwari A., Mamedov F., Grieco M., Suorsa M., Jajoo A., Styring S., … Aro E.M. (2016) Photodamage of iron-sulphur clusters in photosystem i induces non-photochemical energy dissipation. *Nature Plants* **2**.

Trissl H.W. (1997) Determination of the quenching efficiency of the oxidized primary donor of Photosystem I, P700+: Implications for the trapping mechanism. *Photosynthesis Research* **54**, 237–240.

Ueno Y., Shimakawa G., Miyake C. & Akimoto S. (2018) Light-Harvesting Strategy during CO2-Dependent Photosynthesis in the Green Alga Chlamydomonas reinhardtii. *Journal of Physical Chemistry Letters* **9**, 1028–1033.

Verhoeven A. (2014) Sustained energy dissipation in winter evergreens. *New Phytologist* **201**, 57–65.

Welc R., Luchowski R., Kluczyk D., Zubik-Duda M., Grudzinski W., Maksim M., … Gruszecki W.I. (2021) Mechanisms shaping the synergism of zeaxanthin and PsbS in photoprotective energy dissipation in the photosynthetic apparatus of plants. *The Plant Journal* **107**, 418–433.

Wujeska A., Bossinger G. & Tausz M. (2013) Responses of foliar antioxidative and photoprotective defence systems of trees to drought: a meta-analysis. *Tree Physiology* **33**, 1018–1029.

Xu P., Tian L., Kloz M. & Croce R. (2015) Molecular insights into Zeaxanthin-dependent quenching in higher plants. *Scientific reports* **5**, 13679.

Yokono M., Akimoto S. & Tanaka A. (2008) Seasonal changes of excitation energy transfer and thylakoid stacking in the evergreen tree Taxus cuspidata: How does it divert excess energy from photosynthetic reaction center? *Biochimica et Biophysica Acta (BBA) - Bioenergetics* **1777**, 379–387.

Yokono M., Takabayashi A., Akimoto S. & Tanaka A. (2015) A megacomplex composed of both photosystem reaction centres in higher plants. *Nature Communications* **6**, 6675.

Yokono M., Takabayashi A., Kishimoto J., Fujita T., Iwai M., Murakami A., … Tanaka A. (2019) The PSI–PSII Megacomplex in Green Plants. *Plant and Cell Physiology* **60**, 1098–1108.

Zhang S. & Scheller H.V. (2004) Photoinhibition of Photosystem I at Chilling Temperature and Subsequent Recovery in Arabidopsis thaliana. *Plant and Cell Physiology* **45**, 1595–1602.

Zhao Q., Wang G., Ji J., Jin C., Wu W. & Zhao J. (2014) Over-expression of Arabidopsis thaliana β-carotene hydroxylase (chyB) gene enhances drought tolerance in transgenic tobacco. *Journal of Plant Biochemistry and Biotechnology* **23**, 190–198.

Zivcak M., Brestic M., Balatova Z., Drevenakova P., Olsovska K., Kalaji H.M., … Allakhverdiev S.I. (2013) Photosynthetic electron transport and specific photoprotective responses in wheat leaves under drought stress. *Photosynthesis Research* **117**, 529–546.

Figures and Table

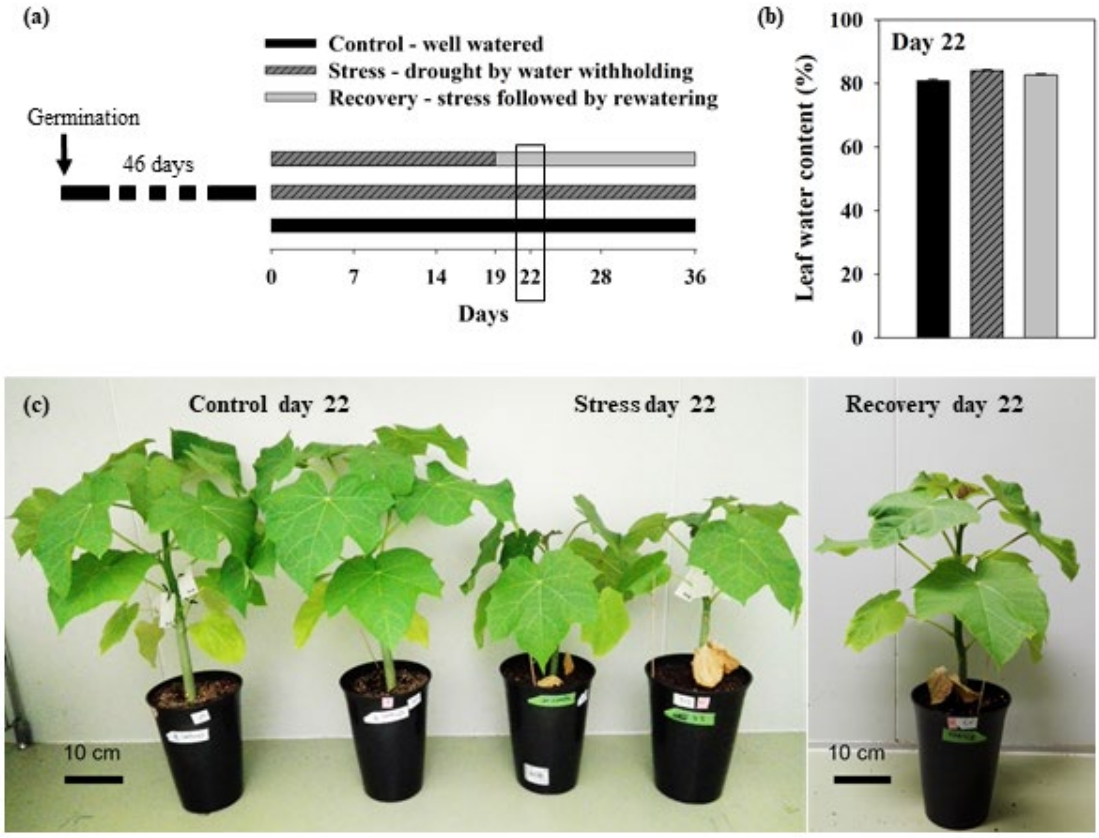

Figure 1. Experimental overview. (a) 46-days-old potted plants were subjected to control (well-watered), stress (drought by water withholding) or stress followed recovery (19-days of stress followed by rewatering). **(b)** Leaf water content and **(c)** morphological aspect of control (well-watered), stress (22-days of drought) and recovery (19-days of drought + 3-days rewatering) plants. Values are means ± SE (n=18 plants per treatment, collected from two independent experiments, except for recovery, in which 4 plants were used). No significant differences were detected in (b) (*p-value≤0.05*).

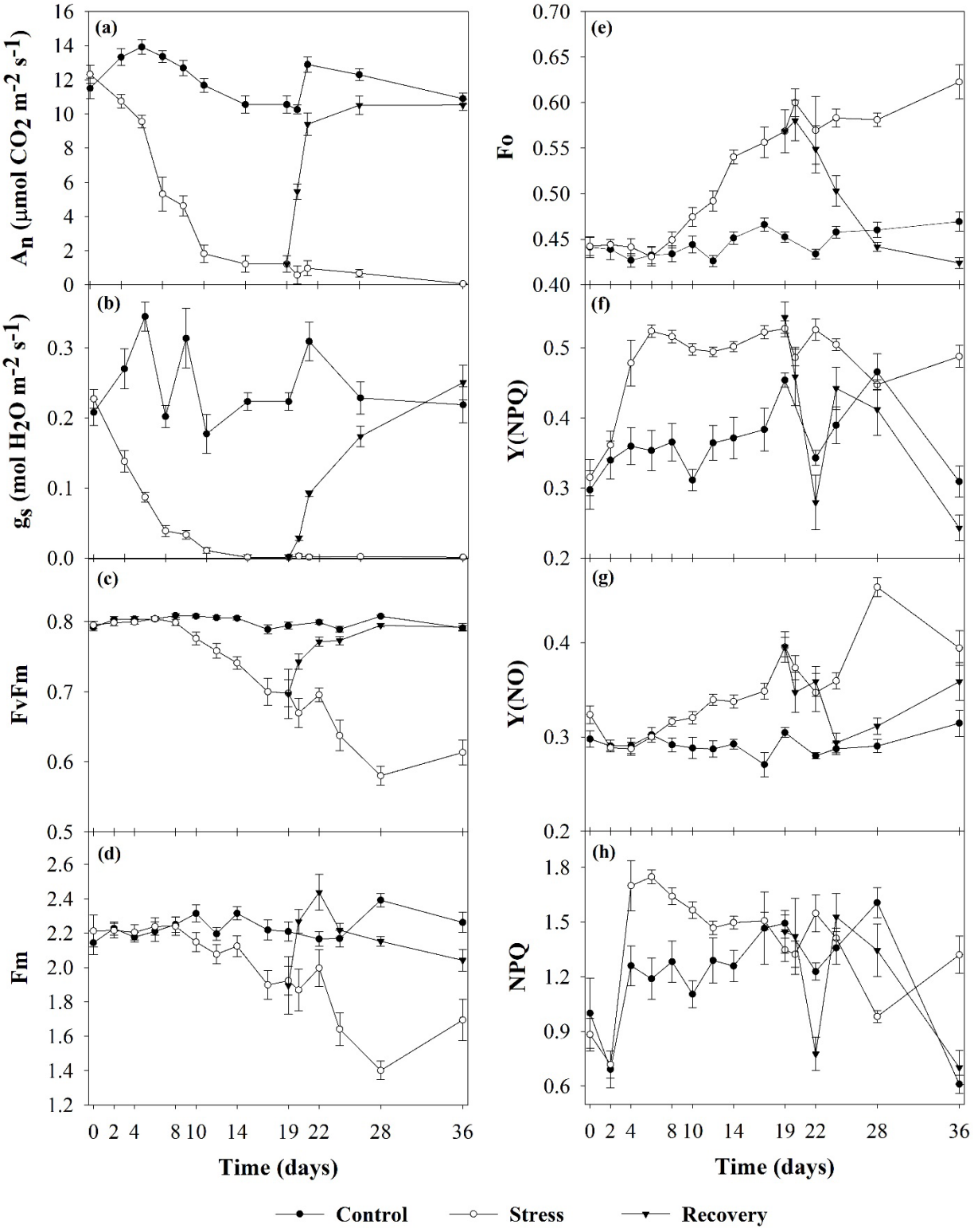

Figure 2. Drought-induced changes on leaf gas exchange and Chl *a* fluorescence. (a) net photosynthesis (A_n), **(b)** stomatal conductance to water vapour (g_s), **(c)** maximum quantum yield of PSII (Fv/Fm), **(d)** maximal fluorescence (Fm)**, (e)** minimal fluorescence (Fo), **(f)** quantum yield of light-induced NPQ (Y(NPQ)), **(g)** quantum yield of non-regulated NPQ (Y(NO)) and **(h)** NPQ measured for *J. curcas* plants subjected to well-watered conditions (Control), water withholding (Stress) or stress for 19-days followed by rewatering (Recovery). **(a-b)** Leaf gas exchange measurements were performed with Tblock=28ºC, [CO_2]=400 ppm, light intensity=400 µmol photons m^{-2} s^{-1} and air flow rate=300 µmol s^{-1}, values are means ± SE (n=4-6 plants). **(c-i)** Chl *a* fluorescence measurements were performed in dark-adapted leaves (≥15 min) using a leaf clip to fix the distance and the leaf area. Fo was determined with a weak measuring light followed by a saturating pulse to estimate Fm. After Fo and Fm determinations, red actinic light (440 µmol photons m^{-2} s^{-1}) was turned on, and a saturating pulse was applied every 20 s to calculate Fm' (maximum fluorescence under light), 14 pulses were performed and the last Fm' measurement was used for the calculation of Y(NPQ) and NPQ. Values are means ± SE (n=18 plants from two independent experiments, except for recovery, in which 4 plants were used).

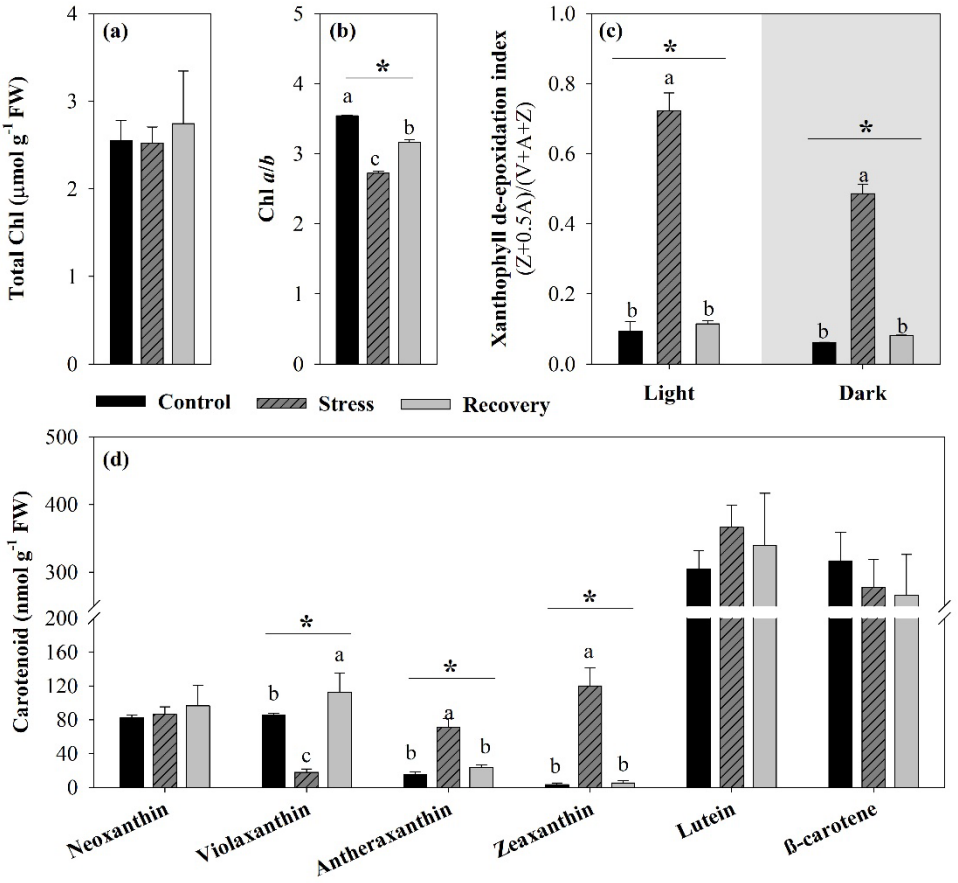

Figure 3. Effect of drought and rewatering on leaf photosynthetic pigment content. **(a)** Total chlorophyll (Chl) content, **(b)** Chl *a* to *b* ratio, **(c)** xanthophyll de-epoxidation index and **d)** carotenoid content of control, stress, and recovery leaves at day 22. For de-epoxidation index leaf samples were collected under light (3 h illumination) or dark (11 h darkness). Values are means ± SE (n=6 plants from two independent experiments). De-epoxidation index was calculated as (Z + 0.5 A)/(V + A+ Z). Z, zeaxanthin; V, violaxanthin and A, antheraxanthin. Different letters within the same group indicate significant differences according to Tukey's test (*p-value≤0.05*).

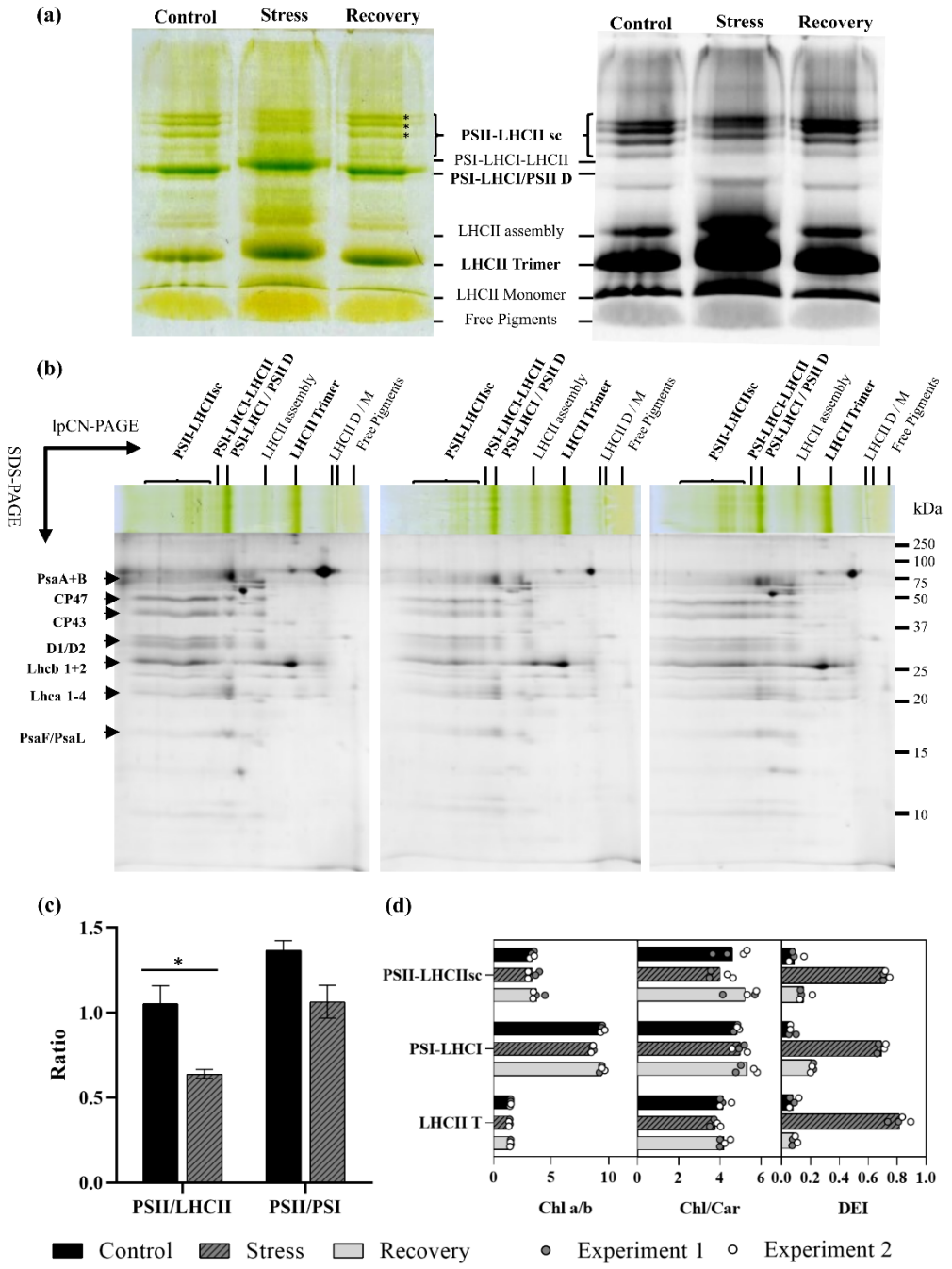

Figure 4. Drought-induced changes in the composition and distribution of thylakoid pigment-binding complexes. (a) Chloroplasts (60 µg of Chl) isolated at day 22 from control, stress, and recovery plants were solubilized with 1% dodecyl-β-maltoside and the pigment-binding complexes separated by large pore clear native PAGE (lpCN-PAGE), fluorescence emission of isolated complexes after excitation with blue light is shown in the right. **(b)** Protein separation of each photosynthetic complex isolated by lpCN-PAGE from control, stress, and recovery samples was performed by second dimension analysis (SDS-PAGE, 14% acrylamide, 6M urea). SDS/PAGE gels were stained with SYPRO Ruby protein stain. The molecular mass in kDa is indicated in the right. The position of major photosystem I (PsaA +PsaB) and II (CP 47, CP43, D1, and D2) reaction center proteins and light-harvesting proteins (Lhca 1 to 4, Lhcb 1 and 2) was highlighted in the figure. The assignment of protein identity was based on the apparent molecular weight in comparison to the literature (Aro *et al.*, 2004; Järvi *et al.*, 2011). **(c)** PSII to LHCII and PSII to PSI ratios. Immunoblot band intensity of CP47 and CP43 for PSII, Lhcb1 and 2 for LHCII and PsaB for PSI were quantified using ImageJ and used for ratio determination (see Fig. S8 for details). Values are means ± SE (n=3 biological samples collected in 2 independent experiments). Significant differences according to the t-test are presented (*p-value≤0.05*). **(d)** Chl *a* to *b* ratio (Chl *a/b*), total Chl to total carotenoid ratio (Chl/Car), and xanthophyll de-epoxidation index (DEI) of isolated PSII-LHCIIsc, PSI-LHCI, and LHCII trimer. The pigment composition of bands enriched with PSII-LHCIIsc (excised bands are highlighted with an asterisk in panel a), PSI-LHCI, and LHCII trimer was determined by HPLC, and pigments normalized by 100 Chls. Bars are means; individual values are presented showing pigment qualifications from 4 independent lpCN-PAGE gels performed after solubilization of thylakoids isolated from two independent experiments. **PSII-LHCIIsc**, Photosystem II supercomplexes; **PSI-LHCI**, Photosystem I and light-harvesting complex I; **PSII-D,** Photosystem II dimer; **LHCII**, light-harvesting complex II; **D/M**, dimer/monomer.

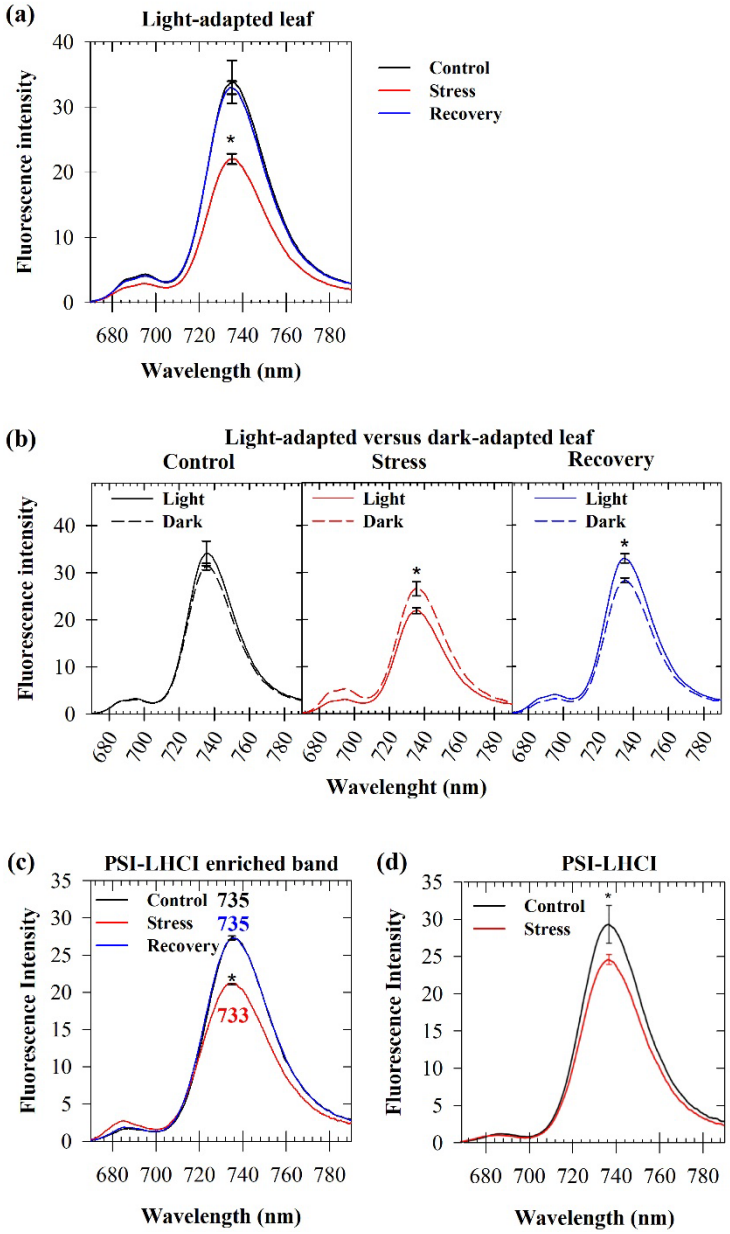

Figure 5. Effect of drought on PSI quantum yield. Low temperature fluorescence (-196 ºC) emission spectra were measured with an Integrated Sphere, samples were excited at 440 nm and the spectra normalized by total number of absorbed excitation photon numbers per sample. **a-b)** Intact leaf discs collected from control, stress, and recovery plants under **(a)** light-adapted (3 h illumination) or **(b)** dark-adapted (11 h dark) conditions. Values are means ± SE (n=3-4 plants from two independent experiments). **(c)** Isolated PSI-LHCI enriched bands (PSI-LHCI/PSII dimer excised from lpCN-PAGE gels, see Fig.4a) from control, stress, and recovery. Values means ± SE (n=3, from two independent experiments). **(d)** Isolated PSI-LHCI (by sucrose density gradient followed by CN-PAGE, see Fig. S10) from control and stress plants. Values are means ± SE (n=3 independent measurements). Significant differences according to Tukey's test are presented (*p-value≤0.05*).

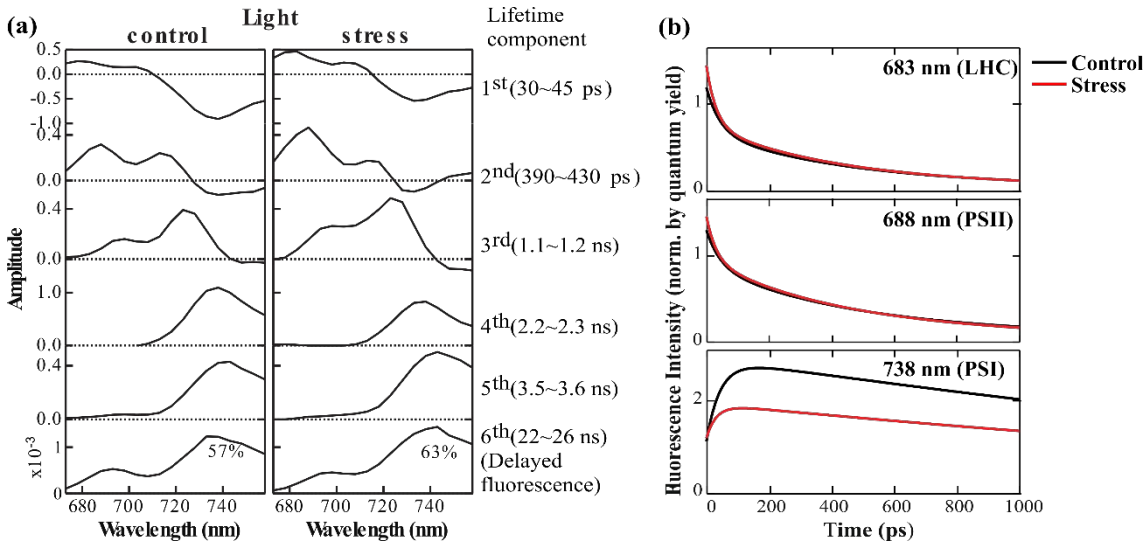

Figure 6. Effect of drought on leaf FDAS. (a) Fluorescence decay-associated spectra (FDAS) of light-adapted (3 h illumination) leaf discs of *J. curcas* plants under control or stress. **(b)** Fluorescence decay curves at 683 nm (top), 688 nm (middle) and 738 (bottom) nm constructed from the FDAS shown in Panel (a). These wavelengths correspond to the typical peak maxima of LHC, PSII and PSI, respectively. Fluorescence intensities are normalized by the results of the quantum yield measurements shown in Fig. 5.

Table 1: Leaf fluorescence decay-associated spectra summary for light-adapted (3 h illumination) leaf discs of *J. curcas* plants under control or stress (3 weeks water-withholding) conditions. **DF**, delayed fluorescence, **PS**, photosystem.

Lifetime fluorescence components	Control	Stress
1st	45 ps	30 ps
2nd	430 ps	390 ps
3rd	1.2 ns	1.1 ns
4th	2.2 ns	2.3 ns
5th	3.6 ns	3.5 ns
6th (DF)	26 ns	22 ns
Mean Lifetime		
PSII : PSI (ns)	1.52 : 2.69	1.14 : 2.80
Delayed fluorescence Intensity (the vibrational band corrected)		
PSII : PSI	0.484 : 1.15	0.325 : 1.34
Estimated spillover ratio	57%	63%